Journal of Neurochemistry

JOURNAL OF NEUROCHEMISTRY | 2016

doi: 10.1111/jnc.13552

ORIGINAL ARTICLE

Neuronal filopodium formation induced by the membrane glycoprotein M6a (Gpm6a) is facilitated by coronin-1a, Rac1, and p21-activated kinase 1 (Pak1)

Anabel Alvarez Juliá, Alberto C. Frasch and Beata Fuchsova

Instituto de Investigaciones Biotecnológicas IIB-INTECH, CONICET-UNSAM, San Martin, Argentina

Abstract

Stress-responsive neuronal membrane glycoprotein M6a (Gpm6a) functions in neurite extension, filopodium and spine formation and synaptogenesis. The mechanisms of Gpm6a action in these processes are incompletely understood. Previously, we identified the actin regulator coronin-1a (Coro1a) as a putative Gpm6a interacting partner. Here, we used co-immunoprecipitation assays with the anti-Coro1a antibody to show that Coro1a associates with Gpm6a in rat hippocampal neurons. By immunofluorescence microscopy, we demonstrated that in hippocampal neurons Coro1a localizes in F-actin-enriched regions and some of Coro1a spots co-localize with Gpm6a labeling. Notably, the over-expression of a dominant-negative form of Coro1a as well as its down-regulation by siRNA interfered with Gpm6a-induced filopodium formation. Coro1a is known to regulate the plasma membrane translocation and activation of small GTPase Rac1. We show that Coro1a co-immunoprecipitates with Rac1 together with Gpm6a. Pharmacological inhibition of Rac1 resulted in a significant decrease in filopodium formation by Gpm6a. The same was observed upon the co-expression of Gpm6a with the inactive GDP-bound form of Rac1. In this case, the elevated membrane recruitment of GDP-bound Rac1 was detected as well. Moreover, the kinase activity of the p21-activated kinase 1 (Pak1), a main downstream effector of Rac1 that acts downstream of Coro1a, was required for Gpm6a-induced filopodium formation. Taken together, our results provide evidence that a signaling pathway including Coro1a, Rac1, and Pak1 facilitates Gpm6a-induced filopodium formation.

Keywords: Coronin-1a, filopodium, hippocampal neuron, membrane glycoprotein M6a, Ras-related C3 botulinum toxin substrate 1 (Rac1), rat.

J. Neurochem. (2016) 10.1111/jnc.13552

Filopodia are thin, actin-rich plasma membrane protrusions that function as sensors for cells to probe their environment. Consequently, filopodia have an important role in cell migration, wound healing, adhesion to the extracellular matrix, and embryonic development (Mattila and Lappalainen 2008; Gallo 2013). In neurons, growth cones contain a large number of filopodia that guide axons and dendrites (Gallo and Letourneau 2004). In addition, filopodia are necessary for the initial neurite formation (Dent *et al.* 2007) and, in dendrites, filopodia act as precursors of dendritic spines (Sekino *et al.* 2007), short bulbous protrusions that form the postsynaptic regions of most excitatory neuronal synapses with an important role in higher brain functions, such as learning and memory. However, in spite of extensive studies, the mechanisms through which specific classes of these structures are generated are still unclear. Variation in the dynamics, length, and positioning of these protrusions in different cells indicates that distinct or differently regulated molecules generate discrete sets of filopodia (Mattila and Lappalainen 2008; Gallo 2013).

Received April 28, 2015; revised manuscript received January 18, 2016; accepted January 19, 2016.

Address correspondence and reprint requests to Beata Fuchsova, Instituto de Investigaciones Biotecnológicas, Universidad Nacional de General San Martin, Av. 25 de Mayo y Francia, Edificio IIB, 1650 San Martin, Buenos Aires, Argentina. E-mail: beata@iibintech.com.ar

Abbreviations used: CA, constitutively activate; Coro1a, coronin-1a; DN, dominant negative; ECL, enhanced chemiluminescence; EGFP, enhanced green fluorescent protein; GAPs, GTPase activating proteins; GDIs, GDP dissociation inhibitors; GEFs, guanine nucleotide exchange factors; Gpm6a, neuronal membrane glycoprotein M6a; N2a, mouse neuro-2a neuroblastoma cell line; Pak1, p21-activated kinase 1; PBS, phosphate-buffered saline; Rac1, Ras-related C3 botulinum toxin substrate 1; RFP, red fluorescent protein; ROI, region of interest; SDS, sodium dodecyl sulfate; TBS, tris-buffered saline; wt, wild type.

Further studies uncovering possible new factors involved in filopodium formation are thus required.

Gpm6a is a membrane glycoprotein abundantly expressed in neurons of CNS, especially in the hippocampus (Yan *et al.* 1996). The functions of Gpm6a in CNS are not fully understood, but the data are accumulating for roles in regulation of filopodium formation, neurite outgrowth and, most likely, synaptogenesis (Lagenaur *et al.* 1992; Mukobata *et al.* 2002; Alfonso *et al.* 2005; Michibata *et al.* 2008; Zhao *et al.* 2008; Fuchsova *et al.* 2009; Brocco *et al.* 2010; Huang *et al.* 2011; Scorticati *et al.* 2011; Mita *et al.* 2015; Formoso *et al.* 2015). Gpm6a over-expression in rat hippocampal neurons as well as in neuronal (N2a, PC12) and non-neuronal cell lines (COS7) induces extensive formation of filopodia. Suppression of endogenous Gpm6a expression by siRNA reduces the number of filopodia and synaptic clusters (Alfonso *et al.* 2005). The filopodia induced by Gpm6a are highly motile and become stabilized upon contact with presynaptic regions (Brocco *et al.* 2010). Mutational analysis identified cysteine residues in the large extracellular domain of Gpm6a to be critical for the process of Gpm6a-induced filopodium formation (Fuchsova *et al.* 2009). Moreover, the localization of Gpm6a in membrane lipid microdomains and the activity of Src kinases and MAPK are required for this process (Scorticati *et al.* 2011).

Gpm6a was originally identified as a stress- and antidepressant-responsive gene in the hippocampus in several animal models of chronic stress (Alfonso *et al.* 2004a,b; Cooper *et al.* 2009; Monteleone *et al.* 2014). In humans, altered hippocampal expression of *GPM6A* have been reported in postmortem brain of depressed suicides (Fuchsova *et al.* 2015). Furthermore, polymorphisms in the *GPM6A* gene sequence have been associated with pathological situations such as schizophrenia (Boks *et al.* 2008), bipolar disorders (Greenwood *et al.* 2012), and claustrophobia (El-Kordi *et al.* 2013). Also, increased *GPM6A* levels resulting from *de novo* duplication of the *GPM6A* gene have been reported in a patient with learning disability and behavioral anomalies (Gregor *et al.* 2014). Notably, this study showed that an increased fraction of patient-derived lymphoblastoid cells formed membrane protrusions compared with cells from healthy controls.

The mechanism by which Gpm6a regulates filopodium formation is not well comprehended. In this article, we describe a central role for the 57 kDa protein Coro1a in this process. This protein belongs to a family of β-propellers, WD40 domain containing proteins. It is expressed in hematopoietic as well as in nervous tissue (Suzuki *et al.* 1995; Nal *et al.* 2004; Jayachandran *et al.* 2014). So far, its function has been mainly studied in immune cells (Pieters *et al.* 2013), and only recently a limited number of studies addressed the function for Coro1a in neuronal cells (Jayachandran *et al.* 2014; Suo *et al.* 2014). Suo *et al.* identified Coro1a as a new effector protein for the nerve growth factor (NGF)-tropomyosin-related kinase type 1 signaling endosome (Suo *et al.* 2014). Another work described a role for Coro1a in cognition and behavior through its activity in modulating cyclic AMP/protein kinase A-dependent synaptic plasticity (Jayachandran *et al.* 2014).

Coro1a is an actin-filament cross-linking and bundling protein that controls the regulation of F-actin structures, cytoskeletal rearrangements, and intracellular membrane transport through multiple modes of action: direct interactions with F-actin, with Arp2/3 complex or regulation of actin depolymerizing factor /cofilin pathway (Rybakin and Clemen 2005; Chan *et al.* 2011; Bustelo *et al.* 2012). Moreover, Coro1a regulates the plasma membrane translocation and activation of small GTPase Rac1 (Castro-Castro *et al.* 2011; Bustelo *et al.* 2012; Ojeda *et al.* 2014). Notably, *Dictyostelium* coronin binds directly the Rac protein through its Cdc42- and Rac-interactive binding motif and Pak1, a main downstream effector of Rac1, was shown to act as a downstream effector of coronin (Swaminathan *et al.* 2014). Therefore, the findings presented above led us to test the hypothesis that the function of Gpm6a leading to filopodium formation depends on Coro1a and involves Rac1/Pak1 signaling pathway.

Materials and methods

Hippocampal cultures, cell line, and plasmid transfections

Dissociated neuronal cultures were prepared from hippocampi of embryonic day 19 Sprague–Dawley rats obtained from the Faculty of Veterinary Sciences (Buenos Aires, Argentina), as described (Brocco *et al.* 2003) (see Data S1 for details). All animal procedures were carried out according to the guidelines of NIH Publications No. 80-23 and approved by the Committee for Care and Use of Laboratory Animals, National University of San Martin (CICUAE-UNSAM No. 03/2011). Mouse neuroblastoma N2a cells were cultured in Dulbecco's modified Eagle's medium with 20% (vol/vol) fetal bovine serum, penicillin, and streptomycin.

Neuronal cultures or N2a cells were transiently transfected with 2 μg of DNA or 50 nM siRNA mixed with 1 μL of Lipofectamine®2000 (Invitrogen, Carlsbad, CA, USA) following the manufacturer's instructions or with 3 μL of polyethylenimine (PEI; Faculty of Pharmacy and Biochemistry, University of Buenos Aires), respectively. For Pak1 inhibition, 10 mM stock solution of 1,1′-disulfanediyldinaphthalen-2-ol (IPA-3; Sigma-Aldrich, St. Louis, MO, USA) was prepared in dimethylsulfoxide (Deacon *et al.* 2008). Transfected neurons were incubated with dimethylsulfoxide, 5 μM and 20 μM IPA-3 for 2 h prior fixation. For Rac1 inhibition, 10 mM stock solution of 6-N-[2-[5-(diethylamino) pentan-2-ylamino]-6-methylpyrimidin-4-yl]-2-methylquinoline-4,6-diamine chloride (NSC 23766; Santa Cruz Biotechnology, Dallas, TX, USA) was prepared in water and transfected neurons were incubated with medium only or 100 μM of NSC 23766 for 24 h prior fixation.

Materials

Mammalian expression plasmids: pRFP-C1 encoding the red fluorescent protein (RFP), pEGFP-C1 (Clontech Laboratories,

Mountain View, CA, USA) encoding the enhanced green fluorescent protein (EGFP), RFP-tagged wild-type (wt) Gpm6a (Gpm6a-RFP) described previously (Alfonso *et al.* 2005), EGFP-tagged wt Coro1a (wtCoro1a-EGFP), and a deletion mutant containing only 5 WD repeats (aa 65-306) of Coro1a [Coro1a(WD1-5)-EGFP] kindly provided by Dr William Trimble (Yan *et al.* 2005), EGFP-tagged Rac1 T17N [Rac1DN-EGFP; Addgene#12982 (Subauste *et al.* 2000)], EGFP-tagged Rac1 Q61L [Rac1CA-EGFP; Addgene#12968 (Subauste *et al.* 2000)], myc-tagged Pak1 K299R [Addgene#12210 (Sells *et al.* 1997)], and myc-tagged Pak1 H83L/H86L [Addgene#12211 (Sells *et al.* 1997)].

siRNAs: siGENOME non-targeting siRNA Pool #2, Coro1a siRNAs targeting either its coding DNA sequence (CDS) [prevalidated in Suo *et al.* (Suo *et al.* 2014)] or its 3′-UTR region (custom designed). Coro1a siRNAs had the following sequence: Coro1a-CDS, sense 5′CCAUGACAGUGCCUAGAAAdTdT, antisense 5′UUUCUAGGCACUGUCAUGGdTdT; Coro1a-UTR, sense 5′GUGGAUAAGACGAAAAUAAdTdT, antisense 5′UUAUUUUCGUCUUAUCCACdTdT. All siRNAs were purchased from Dharmacon.

Primary antibodies: monoclonal anti-Gpm6a rat IgG (1/250; Medical and Biological Laboratories), polyclonal rabbit antibody against C-terminus of Gpm6a (1/3000) developed in our laboratory (Scorticati *et al.* 2011; Fuchsova *et al.* 2015), anti-Coro1a rabbit antiserum (1/6000 for western blot, 1/4000 for immunocytochemistry) kindly provided by Dr Pierre Ferrier (Nal *et al.* 2004), monoclonal anti-c-myc mouse IgG1 (1/1000; Sigma-Aldrich), monoclonal anti-Rac1 mouse antibody (1/1000 for western blot, 1/20 for immunocytochemistry; Cytoskeleton), monoclonal anti-alpha-tubulin mouse IgG1 (1/1000; Sigma-Aldrich), monoclonal anti-MAP2 mouse IgG1 (1/200; Sigma-Aldrich). Secondary antibodies: goat anti-rabbit IgG conjugated to Alexa Fluor (AF) 488 (1/1000; Molecular Probes, Eugene, OR, USA), rhodamine red-conjugated goat anti-rat IgG (1/1000; Jackson Immuno-Research, West Grove, PA, USA), goat anti-rabbit IgG AF 647 (1/1000, Molecular Probes) and goat anti-mouse AF 633 (1/1000; Molecular Probes).

Drugs: Pak1 inhibitor 1,1′-disulfanediyldinaphthalen-2-ol (IPA-3; Sigma-Aldrich); Rac1 inhibitor NSC 23766 (Santa Cruz Biotechnology, Dallas, TX, USA).

Immunocytochemistry

Twenty-four hours or 48 hours (for siRNAs) after transfections, cells were fixed in 4% (wt/vol) paraformaldehyde, 4% (wt/vol) sucrose in phosphate-buffered saline (PBS; 20 min, 25°C). Alternatively, cells were fixed with 90% (vol/vol) methanol in MES buffer [100 mM 2-(N-Morpholino)ethanesulfonic acid (MES), pH 6.9, 1 mM EGTA, 1 mM $MgCl_2$], 5 min, ice-cold. If not indicated otherwise, fixation was followed by permeabilization with 0.1% (vol/vol) Triton X-100 (TX100) in PBS (2 min). Cultures were blocked with 3% (wt/vol) bovine serum albumin (BSA) in PBS (BSA-PBS) with 0.2% (vol/vol) fish skin gelatin followed by incubation with primary antibodies in PBS with 1% (wt/vol) BSA (overnight, 4°C) and secondary antibodies (1 h, 25°C). F-actin was stained with rhodamine red- or AF 488-conjugated phalloidin (1/1000; Molecular Probes) and nuclei with 4′,6-Diamidino-2-phenylindole dihydrochloride (DAPI) (1/3000). Coverslips were mounted in FluorSave Reagent (Calbiochem, San Diego, CA, USA). Fluorescent images were acquired using Nikon E600 microscope with epifluorescence illumination (Plan APO 100× oil, 1.4 NA objective), Nikon Eclipse 80i microscope (Plan APO 60× oil, 1.4 NA, 0.13mmWD objective) with CoolLED pE excitation system or Olympus FluoviewFV1000 confocal laser scanning microscope (Plan APO N 60× oil, 1.42 NA, FN 26.5 objective) with FV10-ASW software.

RNA isolation, cDNA synthesis, and quantitative polymerase chain reaction (qPCR)

Neurons plated in 35 mm plastic Petri dishes (2 DIV) were transfected with siRNAs, cultured and homogenized in 500 µL TRIzol reagent (Invitrogen) 48 h later. Proteins and total RNA were isolated, cDNA was synthesized by retrotranscription, and qPCR reactions were performed on a 7500 Real-Time PCR System from Applied Biosystems (see Data S1 for details).

Immunoprecipitation (IP)

Coro1a was immunoprecipitated from the adult rat hippocampus using the anti-Coro1a rabbit antiserum (see Data S1 for details).

SDS–PAGE and western blotting

The protein samples were loaded on 10% SDS- polyacrylamide gels (18 µg/lane for Input Hipp lysate corresponding to 3% of total protein used per each IP) and transferred to a nitrocellulose membrane by electroblotting. After 2 h of blocking in tris-buffered saline containing 0.2% (vol/vol) Tween-20 and 1% (wt/vol) BSA, the membranes were incubated with the primary antibodies overnight. Antigen–antibody complexes were detected with goat anti-mouse IRDye680 LT (1/20 000), or goat anti-rabbit IRDye800 CW (1/15 000) from LiCor Biosciences using an Odyssey clx infrared imaging system. Alternatively, a horseradish peroxidase-linked purified recombinant Protein A (1/20 000; Pierce) was used according to standard enhanced chemiluminescence western blotting protocol using Super Signal West Pico chemiluminescent substrate (Pierce). Immunoblots were quantified by densitometric analyses using ImageJ software (National Institutes of Health, Bethesda, MA, USA).

Image analysis and Quantification

Co-localization was analyzed using Colocalization Analysis plugins (ImageJ software; see Data S1 for details). Colocalization Highlighter plugin was used to visualize co-localized pixels in each region of interest (ROI) analyzed (Fig. 1c).

To quantify filopodium formation in N2a cells, the percentage of transfected cells showing filopodia was calculated. In primary hippocampal neurons, filopodium density (number of protrusions per 45-µm neurite length as shown in the Fig. 3a) was quantified and results are expressed as fold change in filopodium density over control (see Data S1 for details).

Analysis of confocal images was used to evaluate the localization of Rac1 at cell membrane in neurons over-expressing Gpm6a-RFP or RFP. The distribution of fluorescence intensities along a line drawn across the soma of transfected neurons was measured in each channel. The fluorescence intensity at the cell border was normalized to the average fluorescence intensity in the cytoplasm for each cell (Fig. 6c). On average, 10–15 neurons from each condition done in duplicates were analyzed in two independent experiments.

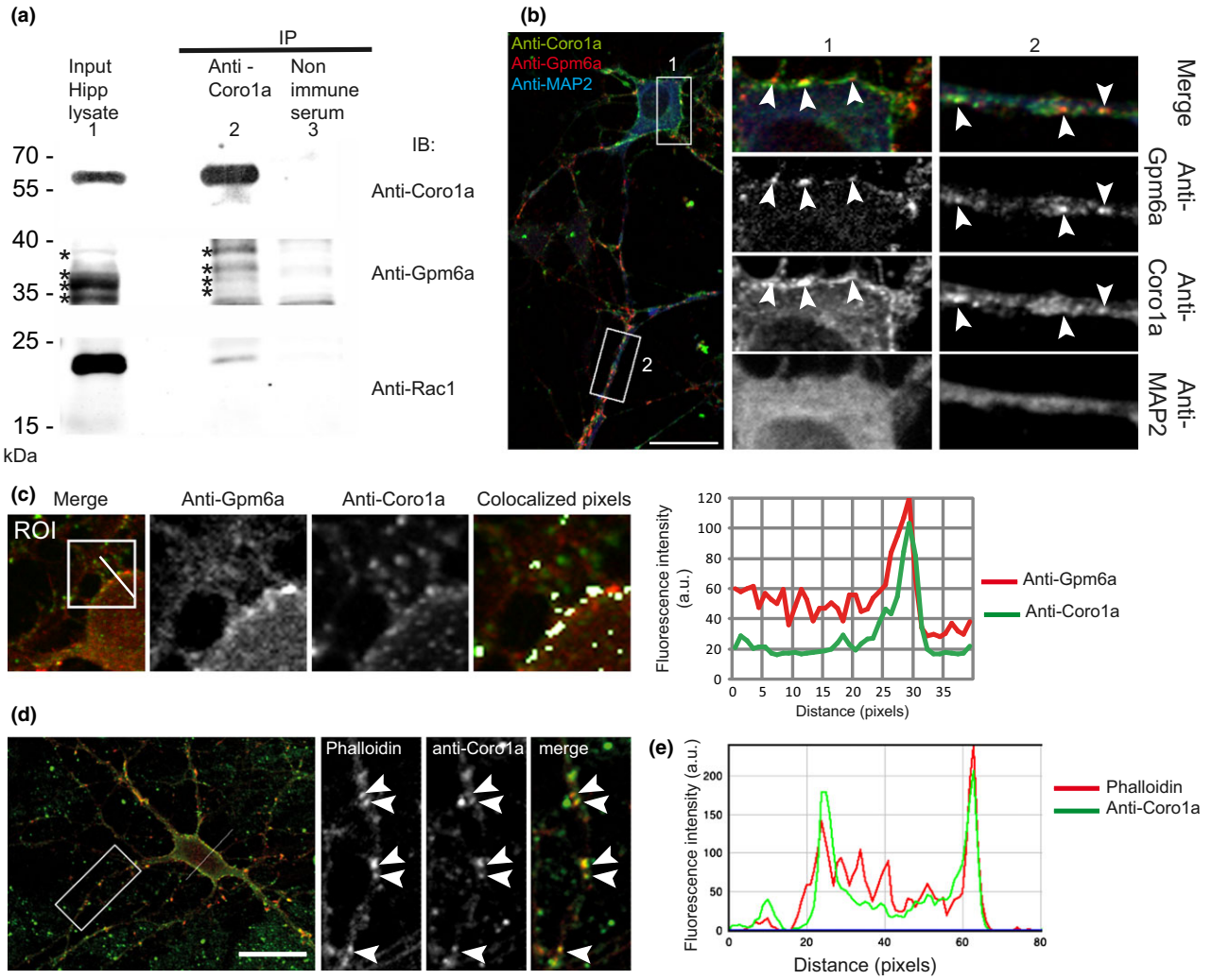

Fig. 1 (a) Gpm6a and Rac1 co-immunoprecipitate with Coro1a from rat hippocampal lysates. Western blot of proteins co-immunoprecipitated from rat hippocampal lysates using anti-Coro1a antibody and probed with anti-Gpm6a, anti-Rac1 and anti-Coro1a antibodies. For this purpose, the membrane (different kDa areas) was cut and incubated with indicated antibodies. Non-immune rabbit serum was used as a control. Gpm6a and Rac1 are present in the anti-Coro1a immunoprecipitate. Bands representing Gpm6a are indicated by stars. (b) Coro1a co-localizes with Gpm6a in hippocampal neurons. Confocal image of hippocampal neurons (4 DIV) co-immunostained with antibodies against Gpm6a (red), Coro1a (green) and dendritic marker MAP2 (blue). A portion of Gpm6a-labeled spots co-localizes with Coro1a (arrowheads; insets 1 and 2). Scale bar, 20 μm. (c) Co-localization was evaluated in ROIs (50 × 50 pixels) as shown in the example. Co-localized pixels (in white) are highlighted with Co-localization Highlighter plugin (ImageJ). Fluorescence intensity profile of anti-Coro1a (green) and anti-Gpm6a (red) along the white line indicated in the ROI shows the overlap of both signals. (d) Confocal image of hippocampal neurons (21 DIV) co-immunostained with anti-Coro1a antibody (green) and F-actin marker phalloidin (red). Co-localizing spots are indicated by arrowheads (maximized view). Scale bar, 20 μm. (e) Fluorescence intensity profile of anti-Coro1a (green) and phalloidin (red) signals along the white line across the soma as indicated in the Fig. 1d shows the overlap of both signals at the juxtamembrane areas of cell.

Statistical data analysis

Calculations and graphs were done with GraphPad Prism 6.00. Group means were analyzed for overall statistical significance using unpaired Student's *t*-test, two-tailed; and when corresponds one-way or two-way ANOVA followed by Tukey multiple comparison test for *post hoc* effects. Results are reported as means + SEM. For all tests, $p \leq 0.05$ was considered statistically significant.

Results

Coro1a associates with Gpm6a in rat hippocampal neurons

Previously, we have identified a 57 kDa protein coronin-1a (Coro1a) to co-immunoprecipitate with Gpm6a (Fuchsova *et al.* 2015). To verify this finding, reciprocal co-immunoprecipitation studies using the anti-Coro1a antibody were

carried out in rat hippocampal lysates. The resulting immunoprecipitates were immunoblotted with anti-Gpm6a and anti-Coro1a antibodies. The endogenous Gpm6a migrating at ~ 35–40 kDa was detected in the hippocampal lysate as well as in the anti-Coro1a immunoprecipitates (Fig. 1a, lanes 1 and 2). As previously observed, Gpm6a migrates by sodium dodecyl sulfate–polyacrylamide gel electrophoresis as multiple bands because of post-translational modifications of the protein such as phosphorylation and glycosylation (Fuchsova *et al.* 2009). In contrast, no Gpm6a was detected in immunoprecipitates when non-immune rabbit serum was used (Fig. 1a, lane 3). In addition to Gpm6a and Coro1a, Rac1 was detected in the anti-Coro1a immunoprecipitates (Fig. 1a, lanes 1 and 2), but not in immunoprecipitates when non-immune rabbit serum was used (Fig. 1a, lane 3).

Previous analysis of Coro1a distribution in the brain by immunohistochemistry and immunoblotting revealed expression throughout different brain regions, including cortex, hippocampus, cerebellar molecular layer, basolateral amygdala, as well as olfactory bulb, with minimal expression in the thalamus (Jayachandran *et al.* 2014). This distribution fits well with the distribution of Gpm6a antigen in the rat brain (Yan *et al.* 1993; Roussel *et al.* 1998; Alfonso *et al.* 2005; Cooper *et al.* 2008). To evaluate the subcellular localization of both proteins, we used primary cultures of rat hippocampal neurons, fixed with methanol, permeabilized, and co-immunostained with antibodies against Gpm6a, Coro1a, and dendritic marker MAP2 and analyzed by confocal microscopy. Consistent with previous findings (Alfonso *et al.* 2005), a punctuate pattern of the endogenous Gpm6a was observed in the plasma membrane and along the neurites (Fig. 1b; red label). Coro1a labeling was detected in the cell soma as well as in spots in the juxtamembrane region and along the neurites (Fig. 1b; green label). We observed that some of these Coro1a-labeled spots were associated with Gpm6a (Fig. 1b, maximized views 1 and 2, arrowheads). Co-localization analysis of confocal images using the Colocalization Analysis plugins of ImageJ revealed that co-localization of these spots with Gpm6a labeling was significant. A value of $R = 0.523$; SEM $\pm$ 0.021 for Pearson's correlation coefficient indicating co-localization was calculated for the analyzed regions of interest (ROI 50 $\times$ 50 pixels; an example of ROI shown in Fig. 1c). This value is significantly higher than the value obtained for randomly overlapped channels ($R = 0.199$; SEM $\pm$ 0.019, $p < 0.0001$ unpaired *t*-test, two-tailed). Mander's colocalization coefficients using the calculated thresholds (tM) were 0.87; SEM$\pm$0.026 for the red channel (tM1) and 0.83; SEM$\pm$0.024 for the green channel (tM2). Figure 1c shows an example of the analyzed ROI, where co-localized pixels are highlighted. The profile plot shows the overlap of the anti-Coro1a (green) and anti-Gpm6a (red) fluorescence intensity peaks along a straight line as indicated in the merged view (Fig. 1c). Taken together, our IP results and co-localization assays suggest that in hippocampal neurons, Coro1a associates with Gpm6a.

Coro1a localizes in F-actin-enriched regions in hippocampal neurons

Coro1a belongs to the group of actin regulators (Rybakin and Clemen 2005; Chan *et al.* 2011; Bustelo *et al.* 2012). Thus, we next evaluated whether Coro1a is localized to F-actin-rich areas in neurons. Costaining of Coro1a with fluorescently labeled F-actin marker phalloidin to visualize cytoskeleton was performed in hippocampal neurons. Confocal microscopy analysis demonstrated that Coro1a-labeled spots co-localized with F-actin accumulations along the neurites (Fig. 1d, arrowheads in maximized view) and with F-actin-rich juxtamembrane regions in the cell body (Fig. 1d and e). The profile plot in Fig. 1e shows the overlap of the anti-Coro1a (green) and phalloidin (red) fluorescence intensity peaks along a straight line intersecting the cell soma as indicated in Fig. 1d. In conclusion, our data confirm that also in hippocampal neurons Coro1a is enriched in F-actin areas consistent with a role for Coro1a in mediating actin dynamics.

Expression of Coro1a dominant-negative form and Coro1a down-regulation interfere with Gpm6a-induced filopodium formation

Previously, we have demonstrated that filopodium formation is one of the processes governed by Gpm6a. Its over-expression was shown to induce an increase in filopodium density in hippocampal neurons, as well as in various cell lines (Alfonso *et al.* 2005). To assess the involvement of Coro1a in this process, we performed over-expression experiments in primary hippocampal neurons and in neuroblastoma cell line N2a.

First, we examined the subcellular localization of the endogenous Coro1a in primary hippocampal neurons over-expressing RFP-tagged Gpm6a (Figure S2). Neurons of 3 DIV were transfected with Gpm6a-RFP or RFP alone as a control and immunocytochemical staining with anti-Coro1a antibody was done. Similar to the endogenous Gpm6a, some Gpm6a-RFP labeled puncta co-localized with the endogenous Coro1a (Figure S2, maximized views, arrowheads). No co-localization was observed in control neurons transfected with RFP alone.

Next, we used a dominant-negative approach by expressing a dominant-negative construct containing only five WD repeats of Coro1a tagged with EGFP [Coro1a(WD1-5); Fig. 2a]. This choice was based on previous studies showing that over-expression of this region interferes with Coro1a function (Mishima and Nishida 1999; Yan *et al.* 2005). Co-expression experiments were first performed in N2a cells. The effect of Coro1a(WD1-5) over-expression on the morphology of Gpm6a-transfected cells was examined. Over-expression of wtCoro1a-EGFP and EGFP alone were

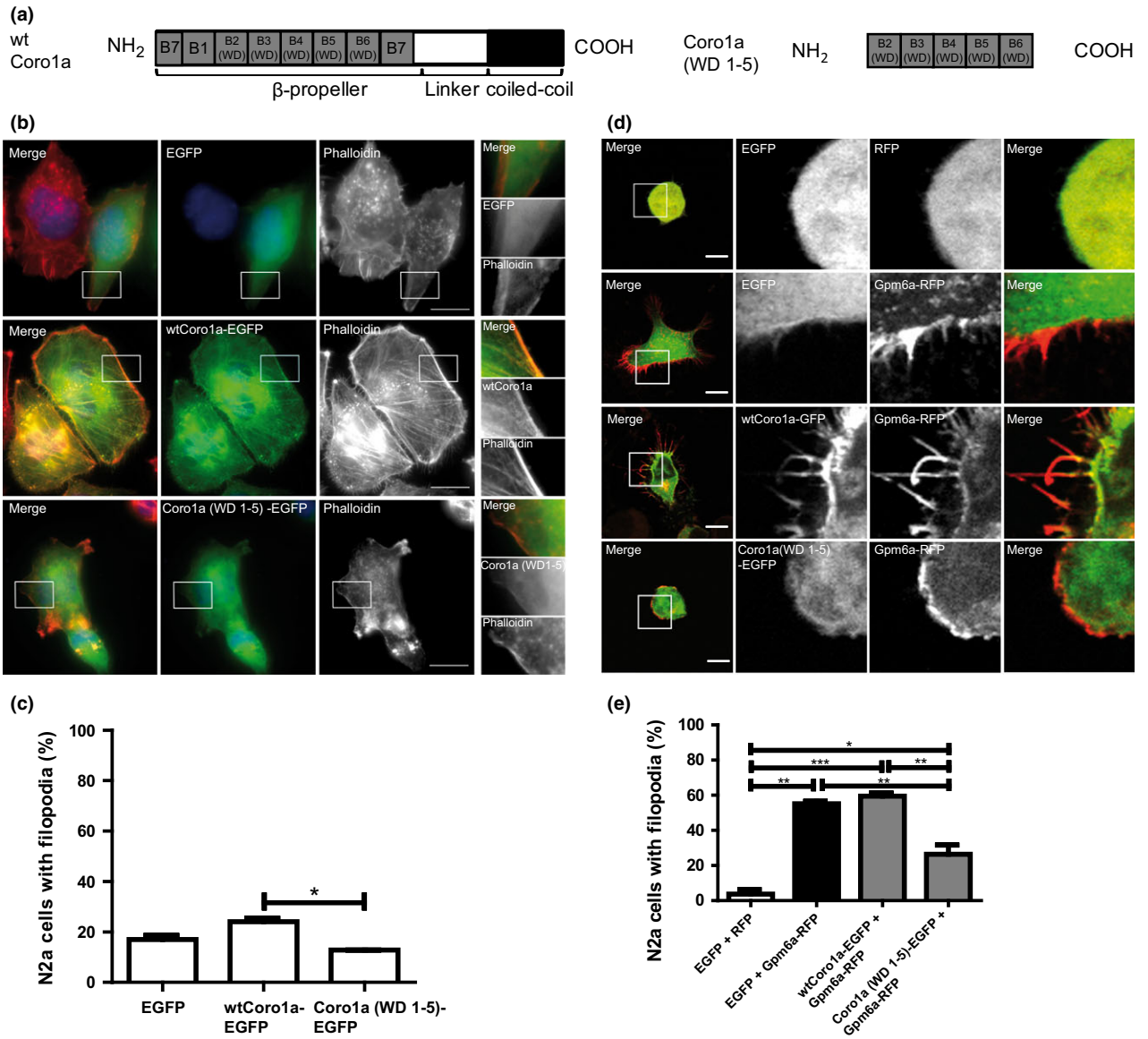

Fig. 2 Over-expression of Coro1a dominant-negative form reduces Gpm6a-induced filopodium formation in N2a cells. (a) Schematic representation of Coro1a domain organization (Gatfield *et al.* 2005). The N-terminal domain containing the seven predicted propeller blades (gray), the linker region (white), and the coiled coil domain (black). Mutant Coro1a(WD1-5) consists of the 5 WD repeat domains (aa 65–306). (b) Localization of wt and mutant Coro1a in N2a cells transfected with indicated vectors and labeled with phalloidin to visualize F-actin cytoskeleton. Scale bar, 10 μm. (c) Over-expression of neither wt nor mutant Coro1a alone induces filopodia formation. The percentage of single transfected N2a cells showing filopodia was quantified in red channel visualizing rhodamine red-phalloidin. On average, 70–100 cells for each transfection condition done in triplicates were analyzed in multiple experiments. Data are means+SEM. One-way ANOVA followed by Tukey multiple comparison test for *post hoc* effects, $*p < 0.05$ wtCoro1a-EGFP versus Coro1a(WD1-5)-EGFP. (d) Co-expression of wt and mutant Coro1a with Gpm6a-RFP in N2a. Wt Coro1a accumulated at the juxtamembrane areas and in filopodial protrusions where Gpm6a was localized (third row). Mutant Coro1a(WD1-5) showed cytoplasmic localization and no overlap with Gpm6a (bottom row). Scale bar, 10 μm. (e) The percentage of double transfected N2a cells with filopodia was quantified in red channel visualizing RFP. On average, 60–120 cells from three to nine groups for each transfection condition were analyzed in multiple experiments. Data are means + SEM. One-way ANOVA followed by Tukey multiple comparison test for *post hoc* effects, $**p < 0.01$ EGFP+RFP versus EGFP+Gpm6a-RFP, $***p < 0.001$ EGFP+RFP versus wtCoro1a-EGFP+Gpm6a-RFP, $*p < 0.05$ EGFP+RFP versus Coro1a(WD1-5)-EGFP+Gpm6a-RFP, $**p < 0.01$ EGFP+Gpm6a-RFP versus Coro1a(WD1-5)-EGFP+Gpm6a-RFP, $**p < 0.01$ wtCoro1a-EGFP+Gpm6a-RFP versus Coro1a(WD1-5)-EGFP+Gpm6a-RFP.

used as controls. Figure 2b shows that upon over-expression, wt Coro1a accumulates in the cytoplasm and at the cell cortex where it co-localizes with F-actin-rich regions as revealed by costaining with phalloidin (Fig. 2b, middle row). Conversely, expression of the central WD repeats region [Coro1a(WD1-5)-EGFP] exhibited a diffuse distribution in the cytoplasm with no accumulation at the juxtamembrane region nor at the F-actin-rich areas (Fig. 2b, bottom row). Over-expression of neither wt nor mutant form of Coro1a induced filopodium formation when compared to EGFP (Fig. 2c). Moreover, the expression of Coro1a(WD1-5) reduced filopodium formation when compared to wtCoro1a-EGFP but not to EGFP alone. Upon co-expression with Gpm6a-RFP, wt Coro1a accumulated at the plasma membrane and in filopodial protrusions where Gpm6a was localized (Fig. 2d, third row). In contrast, Coro1a(WD1-5) showed cytoplasmic localization and no overlap with Gpm6a (Fig. 2d, bottom row). Quantification of the percentage of cells showing filopodia revealed that Gpm6a-induced filopodium formation was significantly lower upon Coro1a (WD1-5) co-expression, while wt Coro1a did not display any effect (Fig. 2e). Co-expression of Gpm6a-RFP with EGFP and RFP with EGFP were used as controls. These results indicate that in the absence of Coro1a function, Gpm6a cannot induce filopodium formation.

To evaluate the effect of the truncated form of Coro1a in cells that normally express Gpm6a, we next examined the effect of Coro1a(WD1-5) over-expression on Gpm6a-induced filopodium formation in primary hippocampal neurons. Neurons of 3 DIV were co-transfected with indicated constructs and fixed 24 h later (Fig. 3a). Co-expression of Gpm6a-RFP with EGFP and RFP with EGFP were used as controls. Figure 3a shows that, as previously reported by our group (Alfonso *et al.* 2005), over-expression of Gpm6a-RFP together with EGFP significantly increased filopodium density comparing to the control co-expression of EGFP with RFP. Similar to N2a cells, co-transfection of wt Coro1a with Gpm6a did not exhibit any effect on Gpm6a-induced increase in filopodium density (Fig. 3a, third row). On the other hand, co-expression of the mutant Coro1a (WD1-5) with Gpm6a inhibited the induction of filopodium formation (Fig. 3a, bottom row). Filopodium density (number of protrusions per 45-μm of neurite length) as shown in the enlarged pictures (Fig. 3a) was quantified. The quantification results in the Fig. 3b show that co-expression with the mutant Coro1a leads to an approximately 50% reduction in Gpm6a-induced filopodia. Filopodium density of neurons co-expressing wt or mutant form of Coro1a with RFP alone did not differ from that of control neurons over-expressing EGFP with RFP (Fig. 3c). Thus, it can be concluded that a

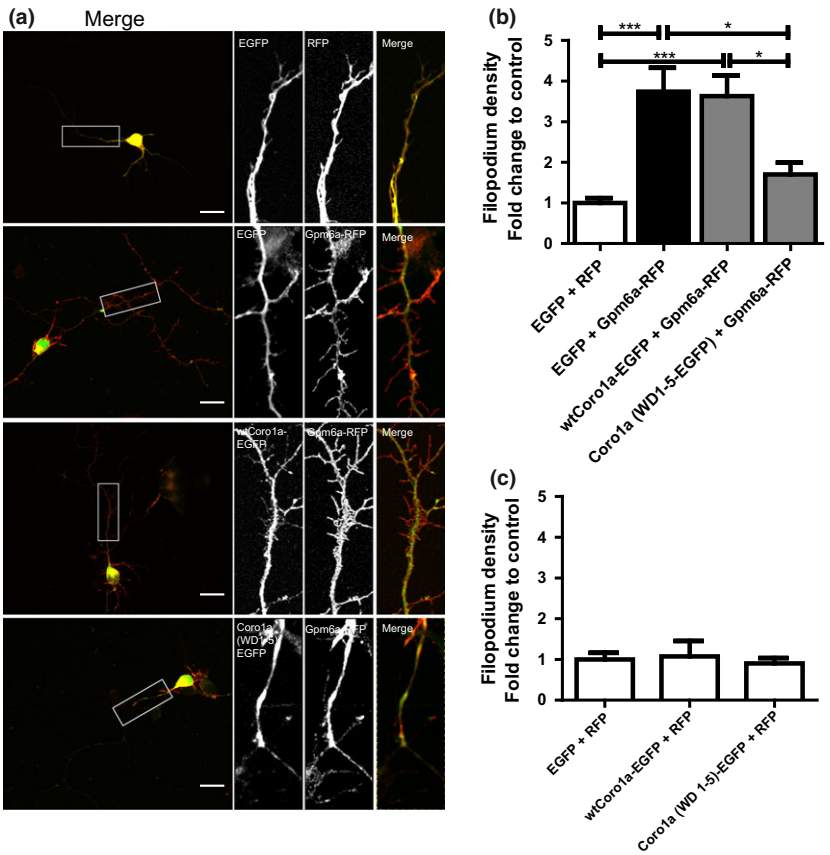

Fig. 3 Over-expression of Coro1a dominant-negative form reduces Gpm6a-induced filopodium formation in hippocampal neurons. (a) Micrographs of hippocampal neurons (4 DIV) co-transfected with indicated vectors. Scale bar, 20 μm. (b) Filopodium density was quantified. Data are means+SEM. 10–20 neurons per group done in duplicates were analyzed in three independent experiments. One-way ANOVA followed by Tukey multiple comparison test for *post hoc* effects, ***$p < 0.001$ EGFP+RFP versus EGFP+Gpm6a-RFP, ***$p < 0.001$ EGFP+RFP versus wtCoro1a-EGFP+Gpm6a-RFP, *$p < 0.05$ EGFP+Gpm6a-RFP versus Coro1a(WD1-5)-EGFP+Gpm6a-RFP, *$p < 0.05$ wtCoro1a-EGFP+Gpm6a-RFP versus Coro1a (WD1-5)-EGFP+Gpm6a-RFP. (c) Control over-expression of neither wt nor mutant Coro1a co-transfected with RFP induces filopodia formation. One-way ANOVA revealed no significant differences between groups.

dominant-negative form of Coro1a that does not distribute to the plasma membrane interferes with Gpm6a-induced filopodium outgrowth in N2a cells as well as in primary hippocampal neurons.

To further support our finding that Gpm6a induces filopodium formation via Coro1a, we have employed siRNA approach to down-regulate Coro1a expression. Primary hippocampal cultures were transfected with two different Coro1a siRNAs targeting its 3′-UTR or CDS region or by control non-targeting siRNA. Efficient down-regulation of Coro1a expression was confirmed by measuring mRNA and protein levels of Coro1a using qPCR and western blot, respectively, only in neurons transfected with siRNA targeting Coro1a CDS region (termed Coro1a siRNA and used in all further experiments). We have detected 40% down-regulation of Coro1a mRNA and approximately 30% down-regulation of Coro1A protein level comparing to control non-targeting siRNA (Fig. 4a). Subsequently, the effect of siRNA down-regulation of Coro1a on Gpm6a-induced filopodium formation was evaluated in hippocampal neurons over-expressing RFP-tagged Gpm6a. Primary hippocampal cultures were co-transfected with siRNA targeting Coro1a or with control non-targeting siRNA and vectors expressing Gpm6a-RFP or RFP alone as a control. Neurons were fixed 48 h later and immunolabeled with anti-Coro1a antibody. Coro1a fluorescence intensity as a measure of Coro1a protein expression in transfected neurons was quantified by immunofluorescence microscopy. We have observed 58% and 48% decreases of Coro1a expression in neurons transfected with Coro1a siRNA and RFP or with Coro1a siRNA and Gpm6a-RFP, respectively, when compared to control non-targeting siRNA (Figure S3). Quantification of filopodium density (number of protrusions per 45-μm of neurite length) showed that this down-regulation led to a statistically significant reduction of 33% in Gpm6a-induced filopodium formation when compared to control non-targeting siRNA (Fig. 4b and c). These results confirm that Coro1a mediates the function of Gpm6a in the formation of filopodia.

Gpm6a-induced filopodium formation involves Rac1

Coro1a is known to regulate plasma membrane localization and activation of Rac1 and its downstream effector Pak1.

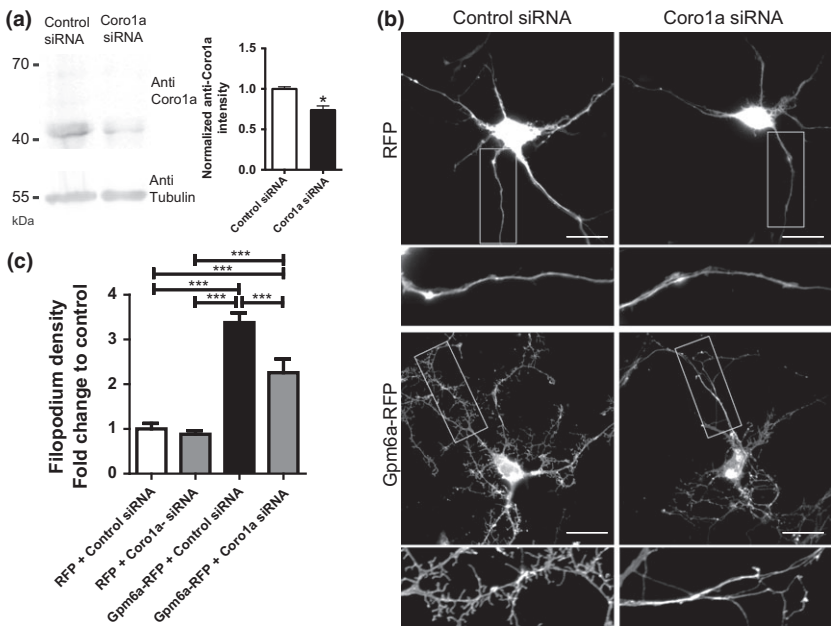

Fig. 4 Down-regulation of Coro1a expression impairs Gpm6a-induced filopodium formation in hippocampal neurons. (a) Western blot shows Coro1a and tubulin protein levels in hippocampal neurons (4 DIV) transfected with control or Coro1a siRNAs. Quantification of Coro1a relative expression levels was done by densitometric analysis of immunoblots from three independent experiments. Coro1a intensity was normalized to tubulin and fold change over control was calculated. Data are means+SEM. Unpaired *t*-test, two-tailed, $*p = 0.0104$ Control siRNA versus Coro1a siRNA. (b) Micrographs of hippocampal neurons (4 DIV) co-transfected with RFP or Gpm6a-RFP and control or Coro1a siRNA 2 days prior fixation. Scale bar, 20 μm. (c) Filopodium density was quantified. Data are means + SEM. 10–20 neurons per group done in triplicates were analyzed in two independent experiments. One-way ANOVA followed by Tukey multiple comparison test for *post hoc* effects, $***p < 0.001$ RFP+Control siRNA versus Gpm6a-RFP+Control siRNA, $***p < 0.001$ RFP+Control siRNA versus Gpm6a-RFP+Coro1a siRNA, $***p < 0.001$ RFP+Coro1a siRNA versus Gpm6a-RFP+Control siRNA, $***p < 0.001$ RFP+Coro1a siRNA versus Gpm6a-RFP+Coro1a siRNA, $***p < 0.001$ Gpm6a-RFP+Control siRNA versus Gpm6a-RFP+Coro1a siRNA.

To evaluate the participation of Rac1 in Gpm6a-induced filopodium formation, we co-transfected hippocampal neurons (3 DIV) with Gpm6a-RFP and EGFP-tagged dominant-negative (DN) Rac1 (T17N). The substitution T17N blocks Rac1 in its inactive GDP-bound form and is thought to exert its dominant-negative effect by sequestering rate-limiting GDP–GTP nucleotide exchange factors necessary for activation of endogenous Rac1 (Ridley *et al.* 1992). Co-expression of Gpm6a-RFP with EGFP and RFP with EGFP were used as controls. Consistent with previously reported observations (Zhang *et al.* 2005), Rac1DN-expressing neurons exhibited smooth dendrites (Fig. 5a, maximized views, third row). Co-expression of this mutant with Gpm6a led to a significant reduction in the number of membrane protrusions comparing to the control neurons expressing Gpm6a with EGFP alone (Fig. 5a, maximized views, second and fourth row; see graph in the Fig. 5b for filopodium density quantification). This indicates that the active form of Rac1 is required for filopodium formation induced by Gpm6a.

To further support our results, we have employed pharmacological inhibition of Rac1 by NSC 23766, a specific inhibitor of the activation of Rac1 GTPase without altering RhoA or Cdc42 activation (Gao *et al.* 2004). Primary hippocampal cultures transfected with EGFP-tagged Gpm6a or EGFP alone as a control were treated with NSC 23766 at 100 μM or with fresh medium (0 μM) for 24 h prior fixation (Fig. 5c). We have found that 100 μM NSC 237666 applied to the neurons blocked 70% of Gpm6a-induced filopodium formation (Fig. 5d). Thus, Rac1 activity is necessary for filopodium formation induced by Gpm6a.

Next, we evaluated whether Gpm6a over-expression affects the localization of Rac1. Hippocampal neurons of 3 DIV were co-transfected with Gpm6a-RFP or RFP and EGFP-tagged Rac1 wt, EGFP-tagged Rac1DN or with EGFP-tagged constitutively activate (CA) Rac1 (Q61L) resistant to GTPase stimulation by Rho GTPase activating proteins (Diekmann *et al.* 1994) to evaluate exogenous Rac1 distribution. Cells were fixed 24 h later. To evaluate endogenous Rac1 distribution, Gpm6a-RFP or RFP expressing neurons were fixed with methanol and immunolabeled with a monoclonal anti-Rac1 antibody. Fluorescence intensity at plasma membrane was analyzed by confocal microscopy as described in Methods section (Fig. 6c). Fig. 6a shows the localization of Rac1 mutants (green) in neurons over-expressing Gpm6a-RFP or RFP. The corresponding plot profiles on the right show the distribution of fluorescence intensities along a line drawn across the somas of transfected neurons. Quantification of fluorescence intensity at plasma membrane depicted in the Fig. 6b revealed significantly higher plasma membrane localization of Rac1DN (green column) in neurons over-expressing Gpm6a when compared to RFP transfected cells. In contrast, Rac1CA localization at the plasma membrane was equally high in Gpm6a or RFP expressing neurons. In addition, we observed co-localization of both Rac1 mutants with Gpm6a accumulations in the cytoplasm. Both Rac1wt-EGFP and endogenous Rac1 were also localized to plasma membrane at a higher level upon Gpm6a-RFP over-expression when compared to control neurons over-expressing RFP (Figure S4). Thus, we conclude that Gpm6a over-expression results in elevated membrane recruitment of Rac1 suggesting a role of Gpm6a in spatial regulation of Rac1 that can contribute significantly to its polarized signaling.

Pak1 activation participates in Gpm6a-induced filopodium formation

The p21-activated kinase 1 (Pak1), one of the major downstream effectors of Rac1 (Kreis and Barnier 2009), has been shown to act downstream of Coro1a in the process of plasma membrane translocation of Rac1 (Castro-Castro *et al.* 2011). At the same time, another study has demonstrated that the kinase activity of Pak1 is necessary for the formation of dendritic spines and protrusions in hippocampal neurons (Zhang *et al.* 2005).

Thus, we next assessed the role of Pak1 in the process of filopodium formation mediated by Gpm6a. Hippocampal neurons of 3 DIV were co-transfected with mutant forms of Pak1 along with Gpm6a-RFP. We used the catalytically inactive form of Pak1 with a single-point mutation in the kinase domain (kinase-dead K299R) as well as the Pak1 form with two-point mutations in the p21-binding domain (H83L/H86L). This double mutant is unable to bind to Cdc42 or Rac1, and has an enhanced kinase activity toward itself and exogenous substrates (Sells *et al.* 1997). Twenty-four hours later, cells were fixed, permeabilized, and immunolabeled with an anti-myc antibody to visualize neurons over-expressing mutant forms of Pak1. Filopodium density was determined as stated previously. Figure 7a shows that Gpm6a co-expression with the kinase-dead Pak1 (K299R) caused a dramatic decrease in the number of Gpm6a-induced filopodia. On the other hand, upon Gpm6a co-expression with the p21-binding domain mutant (H83L/H86L) of Pak1, no effect on filopodium density was observed compared with co-expression of Gpm6a with EGFP (Fig. 7b). To further confirm that Pak1 activity is required for Gpm6a-induced filopodium formation, we used a small molecule, IPA-3, that directly and non-competitively inhibits Group I PAK activity by stabilizing the kinase in a semi-open, catalytically inactive conformation (Deacon *et al.* 2008). Hippocampal neurons of 3 DIV were transfected with Gpm6a-RFP and RFP alone as a control. Twenty-two hours later, cells were treated for 2 h with 5 μM, and 20 μM IPA-3 or vehicle, fixed, and filopodium density was determined. Figure 7c shows that 5 μM and 20 μM IPA-3 applied to the neurons blocked 55% and 88% of Gpm6a-induced filopodium formation,

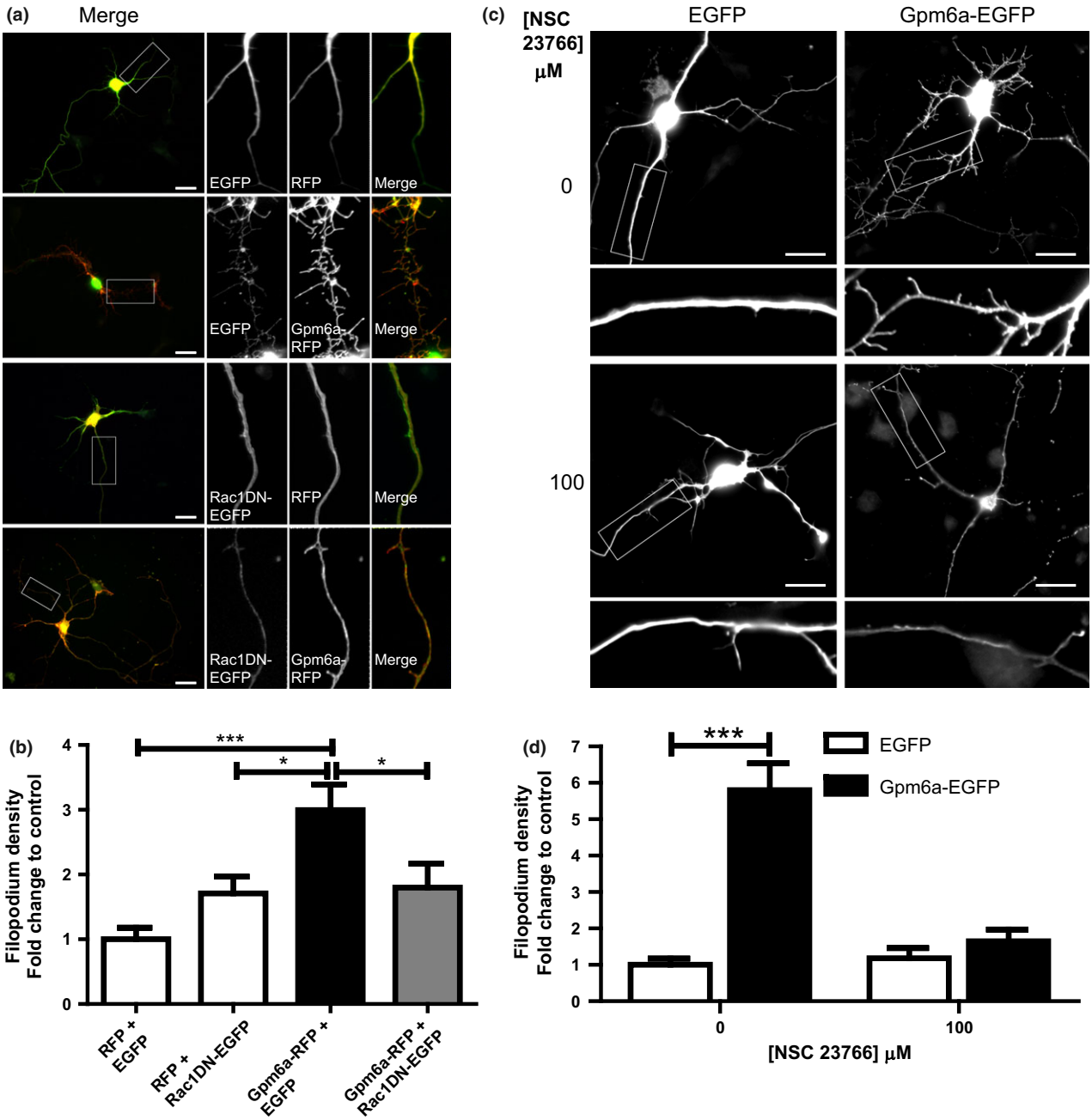

Fig. 5 Inhibition of Rac1 impairs Gpm6a-induced filopodium formation in hippocampal neurons. (a) Micrographs of hippocampal neurons (4 DIV) co-transfected with indicated vectors. Dominant-negative (DN) form of Rac1 (T17N) blocks Rac1 in its inactive GDP-bound form. Scale bar, 20 μm. (b) Filopodium density was quantified. Data are means+SEM. 10–20 neurons per group done in duplicates were analyzed in three independent experiments. One-way ANOVA followed by Tukey multiple comparison test for *post hoc* effects, $*p < 0.05$ EGFP+Gpm6a-RFP versus RFP+Rac1DN-EGFP, $*p < 0.05$ EGFP+Gpm6a-RFP versus Gpm6a-RFP+Rac1DN-EGFP, $***p < 0.001$ EGFP+Gpm6a-RFP versus RFP+EGFP. (c) Micrographs of hippocampal neurons (4 DIV) transfected with EGFP or Gpm6a-EGFP and treated with NSC 23766 (Rac1 inhibitor) at 100 μM or with fresh medium only (0 μM) for 24 h prior fixation. Scale bar, 20 μm. (d) Filopodium density was quantified. Data are means + SEM. 10–20 neurons per group done in duplicates were analyzed in three independent experiment. NSC 23766 blocked Gpm6a-induced filopodium formation. Two-way ANOVA revealed statistically significant *vector x NSC 23766 concentration* interaction ($p < 0.0001$). Tukey multiple comparison test for *post hoc* effect, $***p < 0.001$ EGFP versus Gpm6a-EGFP in non-treated neurons. No difference in filopodium density was found between EGFP and Gpm6a-EGFP when neurons were incubated with 100 μM NSC 23766.

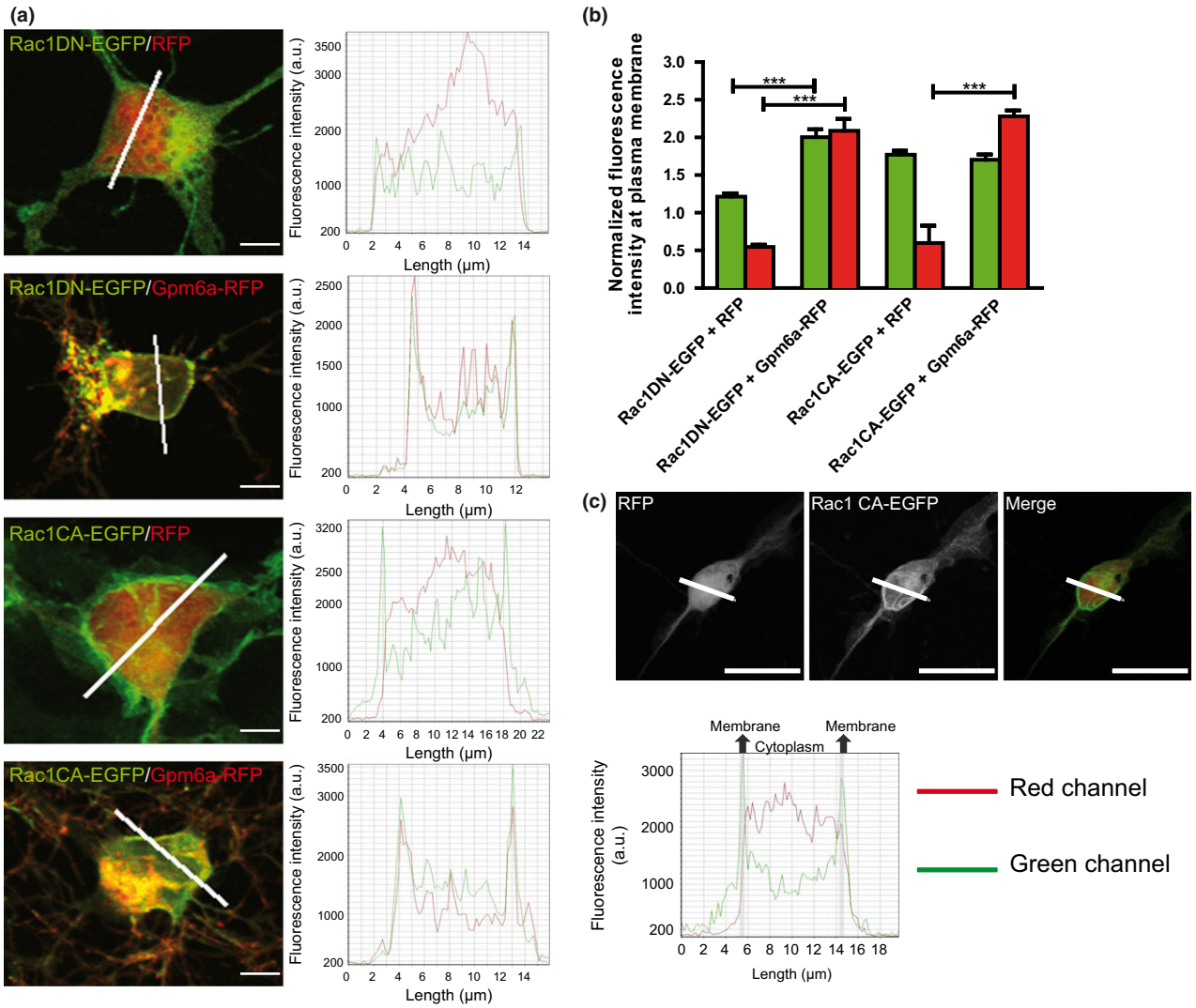

Fig. 6 Localization of Rac1 mutants in neurons over-expressing Gpm6a-RFP. (a) Confocal images of hippocampal neurons (4 DIV) co-transfected with indicated vectors. Dominant-negative (DN) form of Rac1 (T17N) blocks Rac1 in its inactive GDP-bound form. Constitutively activate (CA) form of Rac1 (Q61L) is resistant to GTPase stimulation by Rho GTPase activating proteins. Corresponding fluorescence intensity profiles along a line of approximately 15 μm drawn across the soma as indicated are shown. Scale bar, 5 μm. (b) Quantification of fluorescence intensity at plasma membrane. Fluorescence intensity at plasma membrane was normalized to the average fluorescence in the cytoplasm for each fluorescent protein (Gpm6a-RFP red channel, RFP red channel, Rac1DN-EGFP green channel, Rac1CA-EGFP green channel) as described in Methods section. Data are means + SEM. 10–15 neurons per group done in duplicates were analyzed in two independent experiments. One-way ANOVA followed by Tukey multiple comparison test for *post hoc* effects, $***p < 0.001$ Rac1DN-EGFP+RFP (green channel) versus Rac1DN-EGFP+Gpm6a-RFP (green channel), $***p < 0.001$ Rac1DN-EGFP+RFP (red channel) versus Rac1DN-EGFP+Gpm6a-RFP (red channel), $***p < 0.001$ Rac1CA-EGFP+RFP (red channel) versus Rac1CA-EGFP+Gpm6a-RFP (red channel). (c) Example of the quantification. Confocal image of a neuron co-transfected with RFP and Rac1CA-EGFP. Scale bar, 20 μm. Corresponding fluorescence intensity profile along a line of approximately 15 μm across the soma is shown. In this example, accumulation of Rac1CA-EGFP at plasma membrane can be seen as the peaks of high fluorescence intensity (shaded in gray) at the cell border. Normalized plasma membrane fluorescence intensity of each fluorescent protein was determined as the ratio of fluorescence intensity at the cell border (0.4 μm width shaded in gray) to average fluorescence intensity in the cytoplasm.

respectively. No effect of IPA-3 on RFP-expressing neurons was observed (Fig. 7c). Collectively, these results point to the fact that Pak1 kinase activity is required for Gpm6a-induced filopodium formation in hippocampal neurons.

Discussion

A number of molecules have been implicated in neuronal filopodium formation in a context-dependent manner, suggesting that intricate networks of interconnected signaling

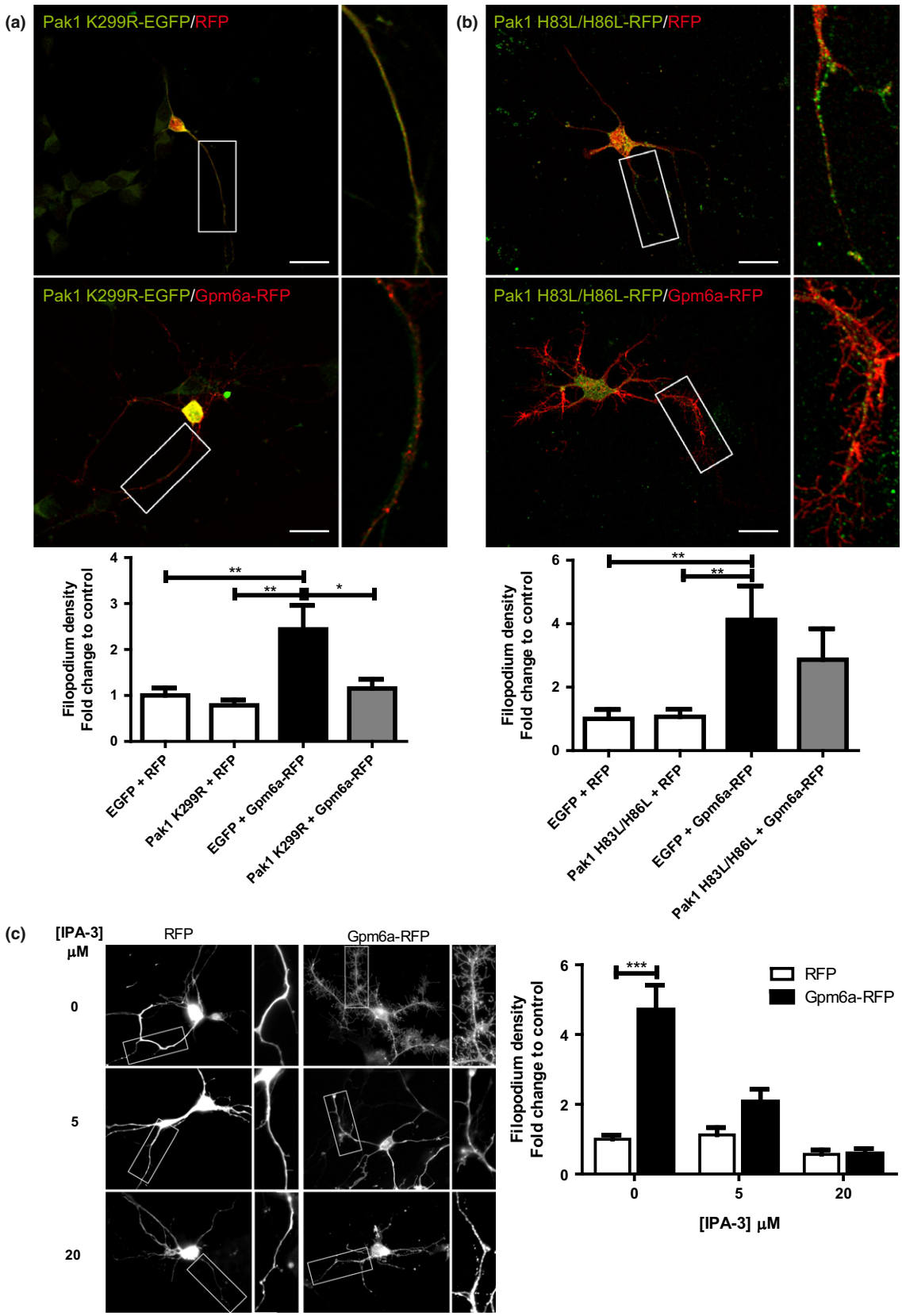
(a)
Pak1 K299R-EGFP/RFP
Pak1 K299R-EGFP/Gpm6a-RFP
(b)
Pak1 H83L/H86L-RFP/RFP
Pak1 H83L/H86L-RFP/Gpm6a-RFP
Filopodium density
Fold change to control
EGFP + RFP
Pak1 K299R + RFP
EGFP + Gpm6a-RFP
Pak1 K299R + Gpm6a-RFP
Pak1 H83L/H86L + RFP
Pak1 H83L/H86L + Gpm6a-RFP
(c)
[IPA-3] μM
RFP
Gpm6a-RFP
[IPA-3] μM

Fig. 7 Pak1 activation participates in Gpm6a-induced filopodium formation. Confocal images of hippocampal neurons (4 DIV) co-transfected with indicated vectors. Scale bar, 20 μm. (a) Kinase-dead Pak1 (K299R) causes a significant decrease in the number of Gpm6a-induced filopodia. Filopodium density was quantified. Data are means+SEM. 10–20 neurons per group done in duplicates were analyzed in three independent experiments. One-way ANOVA followed by Tukey multiple comparison test for *post hoc* effect, $*p < 0.05$ EGFP+Gpm6a-RFP versus Pak1K299R+Gpm6a-RFP, $**p < 0.01$ EGFP+Gpm6a-RFP versus EGFP+RFP, $**p < 0.01$ EGFP+Gpm6a-RFP versus Pak1K299R+RFP. (b) The p21-binding domain mutant (H83L/H86L) of Pak1 shows no effect on Gpm6a-induced filopodium density. Filopodium density was quantified. Data are means+SEM. 10–20 neurons per group done in duplicates were analyzed in two independent experiments. One-way ANOVA followed by Tukey comparison test, $**p < 0.01$ EGFP+Gpm6a-RFP versus EGFP+RFP, $**p < 0.01$ EGFP+Gpm6a-RFP versus Pak1H83L/H86L+RFP. (c) Micrographs of hippocampal neurons (4 DIV) transfected with RFP or Gpm6a and treated with IPA-3 (Pak1 inhibitor) at 5, 20, or 0 μM [vehicle dimethylsulfoxide] for 2 h prior fixation. Filopodium density was quantified. Data are means + SEM. 10–20 neurons per group done in duplicates were analyzed in three independent experiment. IPA-3 blocked Gpm6a-induced filopodium formation. Two-way ANOVA revealed statistically significant *vector x IPA-3 concentration* interaction ($p < 0.0001$). Tukey multiple comparison test for *post hoc* effect, $***p < 0.001$ RFP versus Gpm6a-RFP in neurons treated with vehicle. No difference in filopodium density was found between RFP and Gpm6a-RFP when IPA-3 was applied at either concentration.

pathways converge to regulate actin dynamics. This complexity is not surprising, given the fact that in the nervous system, filopodia underlie many major morphogenetic events (Mattila and Lappalainen 2008; Gallo 2013). In previous studies, we and others have demonstrated that the neuronal membrane glycoprotein Gpm6a is a key modulator for neurite outgrowth, filopodium/spine formation, and synaptogenesis (Lagenaur *et al.* 1992; Mukobata *et al.* 2002; Alfonso *et al.* 2005; Michibata *et al.* 2008; Zhao *et al.* 2008; Fuchsova *et al.* 2009; Brocco *et al.* 2010; Huang *et al.* 2011; Scorticati *et al.* 2011; Mita *et al.* 2015; Formoso *et al.* 2015). In order to clarify the mechanism that mediates Gpm6a morphogenetic effects, we searched for proteins that form complexes with endogenous Gpm6a in rat hippocampus. Using immunoprecipitation experiments followed by mass spectrometry, the cytoskeletal regulator Coro1a was identified as one of the proteins that associate with Gpm6a (Fuchsova *et al.* 2015). In this study, we provide evidence that Coro1a mediates the function of Gpm6a in the formation of filopodia possibly through a process that involves Rac1 and Pak1.

First, we demonstrated that in rat hippocampus, the endogenous Gpm6a specifically associates with Coro1a as revealed by the co-immunoprecipitation assays. Indeed, previous analysis of neuronal distribution of both proteins suggests that their expression correlates throughout different brain regions, including the hippocampus (Yan *et al.* 1993; Roussel *et al.* 1998; Alfonso *et al.* 2005). Here, our subcellular localization studies in rat hippocampal neurons confirmed a co-localization of a portion of Coro1a-labeled spots with endogenous Gpm6a. Moreover, Coro1a co-localized with F-actin-rich areas along the neurites and in the juxtamembrane regions of primary hippocampal neurons. This is in accordance with the immunofluorescence microscopy studies done in hematopoietic cells that revealed co-localization of Coro1a with the cortical F-actin-rich areas at the plasma membrane (Gatfield *et al.* 2005) and consistent with the previously published role for Coro1a in mediating actin dynamics in a variety of processes in immune cells (Rybakin and Clemen 2005; Chan *et al.* 2011; Bustelo *et al.* 2012). Gatfield *et al.* (2005) have demonstrated that Coro1a is organized into three domains: an N-terminal, WD repeat-containing β-propeller connected by a linker region to a coiled coil (Fig. 2a). The N-terminal β-propeller domain mediates plasma membrane binding, while interaction with F-actin cytoskeleton occurs via a stretch of positively charged residues in the linker region exclusively upon trimerization mediated via the coiled coil domain (Gatfield *et al.* 2005). In their study, the authors suggested that by linking the plasma membrane to the underlying actin cytoskeleton in immune cells, Coro1a may facilitate the integration of extracellular signals with F-actin remodeling. Nevertheless, the binding partners of the N-terminal of Coro1a at the plasma membrane remain unknown. In this sense, Gpm6a might act as the N-terminal binding partner of Coro1a, although it remains to be established whether the interaction between Gpm6a and Coro1a is direct and which part of the molecule mediates the binding.

Next, we asked whether Coro1a participates in the process of filopodium formation triggered by Gpm6a over-expression. Observed co-localization of the endogenous Coro1a with over-expressed Gpm6a in rat hippocampal neurons suggested its involvement. Subsequent interference with this process using the expression of a dominant-negative form of Coro1a or by Coro1a down-regulation using the siRNA approach clearly demonstrated that Coro1a mediates Gpm6a-induced filopodium formation. Thus, Coro1a may link Gpm6a with F-actin remodeling. In addition, we observed that the small GTPase Rac1 was present in the anti-Coro1a immunoprecipitates and that the Gpm6a-induced filopodium formation was also dependent on Rac1. Its pharmacological inhibition or co-expression of Rac1-inactive GDP-bound form led to a significant reduction in the number of membrane protrusions. Our results are in agreement with the known function of Coro1a in the regulation of the plasma membrane translocation and activation of Rac1 (Castro-Castro *et al.* 2011; Bustelo *et al.* 2012; Ojeda *et al.* 2014) as well as with a critical role of Rac1 in the maintenance and reorganization of dendritic structures in maturing neurons

(Nakayama *et al.* 2000; Zhang *et al.* 2003; Vadodaria *et al.* 2013). Coro1a over-expression has been shown to induce the F-actin-dependent translocation and activation of Rac1, but not that of more distantly related members of Rho family of small GTPases such as RhoA and Cdc42. Conversely, Coro1a inactivation led to ineffective activation of Rac1 and Rac1-downstream routes (Castro-Castro *et al.* 2011). Thus, altered Rac1 activation appears a likely mediator of Gpm6a effects.

However, this is in contrast with our previous observation that no activation or inhibition of Rac1 by Gpm6a could be detected in N2a and COS7 cells (Alfonso *et al.* 2005). One possible explanation of this discrepancy is that Rac1 involvement in Gpm6a-induced filopodium formation is cell type specific and acts only in hippocampal neurons. Another possibility is that while activated Rac1 is necessary for Gpm6a-induced filopodium formation, Gpm6a by itself acts as a scaffolding protein that modulates Rac1 translocation to plasma membrane, but does not affect GTP loading. By anchoring Coro1a at the plasma membrane, it could make possible the subsequent activation of Rac1 by guanine nucleotide exchange factors in the correct subcellular localization.

Indeed, Rac1 activation involves two steps: translocation to plasma membrane and nucleotide exchange. Previous studies have shown that these are separable events (Moissoglu *et al.* 2006). The spatial regulation of membrane translocation of Rac1 is not directly dependent on the activation (the nucleotide-bound) state of the molecule. Rac1 recruitment to membrane precedes its interaction with protein factors such as guanine nucleotide exchange factors that promote Rac1 activation through the exchange of GDP for GTP (Das *et al.* 2015). Accordingly, in our experiments, Gpm6a over-expression resulted in elevated membrane recruitment of GDP-bound Rac1 thus indicating a role of Gpm6a in spatial regulation of Rac1 translocation rather than in nucleotide exchange. Our observation is consistent with data showing that Rac1 recruitment to membrane precedes nucleotide exchange of GDP for GTP.

It is tempting to speculate that upon Gpm6a over-expression, mislocalized active signaling complexes may lead to an overabundance of filopodial protrusions with consequences for neuronal remodeling and connectivity. Indeed, the spatial restriction of signaling ensures localized and polarized intracellular responses to extracellular cues. The best-known regulators of the dynamic segregation of the inactive and active Rac1 pools in different subcellular localizations are the Rho GDP dissociation inhibitors (RhoGDIs) that sequester GDP–Rac1 in the cytosol (DerMardirossian and Bokoch 2005). Alternatively, recent studies suggest that Rac1 activity is regulated by endocytosis, localization to endosomes and subsequent recycling to the plasma membrane. This guarantees localized signaling, leading to the formation of actin-based migratory protrusions. Rac1 recruitment to these endomembranes occurs independently of the nucleotide-bound state (Palamidessi *et al.* 2008). Notably, in our confocal studies, we observed that the spots of over-expressed Gpm6a in cell soma co-localized with Coro1a (Figure S2, arrowheads) as well as with both Rac1 mutants (Rac1DN and Rac1CA; Fig. 6a). It would, therefore, be of interest to determine the origin of these punctuate membrane structures and identify whether they form components of distinct membrane trafficking pathways. In this context, the roles for Gpm6a and Coro1a in endocytosis can be highly relevant. For example, Gpm6a has been shown to act as a scaffolding molecule in the regulation of endocytosis and recycling of G protein-coupled receptors such as the μ-opioid receptor (Wu *et al.* 2007). On the other hand, Coro1a was shown to mediate stability, recycling, and re-internalizing the signaling endosome induced by neuronal exposure to NGF (Suo *et al.* 2014).

The major downstream effector of Rac1, Pak1 (Kreis and Barnier 2009), acts downstream of Coro1a in the process of plasma membrane translocation of Rac1 (Castro-Castro *et al.* 2011). In addition, a direct interaction of coronin and Pak was observed in *Dictyostelium*, where Pak and coronin also partially co-localized (Swaminathan *et al.* 2014). In hippocampal neurons, the kinase activity of Pak1 has been shown previously to be required for the formation of dendritic spines and protrusions (Zhang *et al.* 2005). Consistent with the aforementioned studies, we observed that Pak1 activation is required for Gpm6a-induced filopodium formation. Taken together, our results point to a Gpm6a-induced filopodium formation by signaling pathway that involves Coro1a, Rac1, and Pak1, possibly via spatial regulation of the subcellular localization of its components.

Acknowledgments and conflict of interest disclosure

We are grateful to Dr William Trimble for Coro1a expression vectors and to Dr Pierre Ferrier for the anti-Coro1a antibody. This study was supported by ANPCyT grants (ACF, BF) and by CONICET and ISN-CAEN grants (BF). AAJ is recipient of CONICET doctoral fellowship. BF and ACF are CONICET researchers. The funding sources had no role in study design, acquisition, and interpretation of data or writing of the report. The authors have no conflict of interest to declare.

Supporting information

Additional supporting information may be found in the online version of this article at the publisher's web-site:

Figure S1. Over-expression of Gpm6a induces filopodium formation in hippocampal neurons.

Figure S2. Puncta of over-expressed Gpm6a co-localize with a portion of Coro1a-labeled spots in hippocampal neurons.

Figure S3. Down-regulation of Coro1a by siRNA approach in neurons over-expressing RFP or Gpm6a-RFP.

Figure S4. Localization of wt Rac1 in neurons over-expressing Gpm6a-RFP.

Data S1. Material and Methods.

References

Alfonso J., Aguero F., Sanchez D. O., Flugge G., Fuchs E., Frasch A. C. and Pollevick G. D. (2004a) Gene expression analysis in the hippocampal formation of tree shrews chronically treated with cortisol. *J. Neurosci. Res.* **78**, 702–710.

Alfonso J., Pollevick G. D., Van Der Hart M. G., Flugge G., Fuchs E. and Frasch A. C. (2004b) Identification of genes regulated by chronic psychosocial stress and antidepressant treatment in the hippocampus. *Eur. J. Neurosci.* **19**, 659–666.

Alfonso J., Fernandez M. E., Cooper B., Flugge G. and Frasch A. C. (2005) The stress-regulated protein M6a is a key modulator for neurite outgrowth and filopodium/spine formation. *Proc. Natl Acad. Sci. USA* **102**, 17196–17201.

Boks M. P., Hoogendoorn M., Jungerius B. J., Bakker S. C., Sommer I. E., Sinke R. J., Ophoff R. A. and Kahn R. S. (2008) Do mood symptoms subdivide the schizophrenia phenotype? Association of the GMP6A gene with a depression subgroup. *Am. J. Med. Genet. B Neuropsychiatr. Genet.* **147B**, 707–711.

Brocco M., Pollevick G. D. and Frasch A. C. (2003) Differential regulation of polysialyltransferase expression during hippocampus development: implications for neuronal survival. *J. Neurosci. Res.* **74**, 744–753.

Brocco M. A., Fernandez M. E. and Frasch A. C. (2010) Filopodial protrusions induced by glycoprotein M6a exhibit high motility and aids synapse formation. *Eur. J. Neurosci.* **31**, 195–202.

Bustelo X. R., Ojeda V., Barreira M., Sauzeau V. and Castro-Castro A. (2012) Rac-ing to the plasma membrane: the long and complex work commute of Rac1 during cell signaling. *Small GTPases* **3**, 60–66.

Castro-Castro A., Ojeda V., Barreira M. *et al.* (2011) Coronin 1A promotes a cytoskeletal-based feedback loop that facilitates Rac1 translocation and activation. *EMBO J.* **30**, 3913–3927.

Chan K. T., Creed S. J. and Bear J. E. (2011) Unraveling the enigma: progress towards understanding the coronin family of actin regulators. *Trends Cell Biol.* **21**, 481–488.

Cooper B., Werner H. B. and Flugge G. (2008) Glycoprotein M6a is present in glutamatergic axons in adult rat forebrain and cerebellum. *Brain Res.* **1197**, 1–12.

Cooper B., Fuchs E. and Flugge G. (2009) Expression of the axonal membrane glycoprotein M6a is regulated by chronic stress. *PLoS ONE* **4**, e3659.

Das S., Yin T., Yang Q., Zhang J., Wu Y. I. and Yu J. (2015) Single-molecule tracking of small GTPase Rac1 uncovers spatial regulation of membrane translocation and mechanism for polarized signaling. *Proc. Natl Acad. Sci. USA* **112**, E267–E276.

Deacon S. W., Beeser A., Fukui J. A., Rennefahrt U. E., Myers C., Chernoff J. and Peterson J. R. (2008) An isoform-selective, small-molecule inhibitor targets the autoregulatory mechanism of p21-activated kinase. *Chem. Biol.* **15**, 322–331.

Dent E. W., Kwiatkowski A. V., Mebane L. M. *et al.* (2007) Filopodia are required for cortical neurite initiation. *Nat. Cell Biol.* **9**, 1347–1359.

DerMardirossian C. and Bokoch G. M. (2005) GDIs: central regulatory molecules in Rho GTPase activation. *Trends Cell Biol.* **15**, 356–363.

Diekmann D., Abo A., Johnston C., Segal A. W. and Hall A. (1994) Interaction of Rac with p67phox and regulation of phagocytic NADPH oxidase activity. *Science* **265**, 531–533.

El-Kordi A., Kastner A., Grube S. *et al.* (2013) A single gene defect causing claustrophobia. *Transl. Psychiatry.* **3**, e254.

Formoso K., Billi S. C., Frasch A. C. and Scorticati C. (2015) Tyrosine 251 at the C-terminus of neuronal glycoprotein M6a is critical for neurite outgrowth. *J. Neurosci. Res.* **93**, 215–229.

Fuchsova B., Fernandez M. E., Alfonso J. and Frasch A. C. (2009) Cysteine residues in the large extracellular loop (EC2) are essential for the function of the stress-regulated glycoprotein M6a. *J. Biol. Chem.* **284**, 32075–32088.

Fuchsova B., Alvarez Julia A., Rizavi H. S., Frasch A. C. and Pandey G. N. (2015) Altered expression of neuroplasticity-related genes in the brain of depressed suicides. *Neuroscience* **299**, 1–17.

Gallo G. (2013) Mechanisms underlying the initiation and dynamics of neuronal filopodia: from neurite formation to synaptogenesis. *Int. Rev. Cell Mol. Biol.* **301**, 95–156.

Gallo G. and Letourneau P. C. (2004) Regulation of growth cone actin filaments by guidance cues. *J. Neurobiol.* **58**, 92–102.

Gao Y., Dickerson J. B., Guo F., Zheng J. and Zheng Y. (2004) Rational design and characterization of a Rac GTPase-specific small molecule inhibitor. *Proc. Natl Acad. Sci. USA* **101**, 7618–7623.

Gatfield J., Albrecht I., Zanolari B., Steinmetz M. O. and Pieters J. (2005) Association of the leukocyte plasma membrane with the actin cytoskeleton through coiled coil-mediated trimeric coronin 1 molecules. *Mol. Biol. Cell* **16**, 2786–2798.

Greenwood T. A., Akiskal H. S., Akiskal K. K. and Kelsoe J. R. (2012) Genome-wide association study of temperament in bipolar disorder reveals significant associations with three novel Loci. *Biol. Psychiatry* **72**, 303–310.

Gregor A., Kramer J. M., van der Voet M., Schanze I., Uebe S., Donders R., Reis A., Schenck A. and Zweier C. (2014) Altered GPM6A/M6 dosage Impairs cognition and causes phenotypes responsive to cholesterol in human and drosophila. *Hum. Mutat.* **35**, 1495–1505.

Huang K. Y., Chen G. D., Cheng C. H. *et al.* (2011) Phosphorylation of the zebrafish M6Ab at serine 263 contributes to filopodium formation in PC12 cells and neurite outgrowth in zebrafish embryos. *PLoS ONE* **6**, e26461.

Jayachandran R., Liu X., Bosedasgupta S. *et al.* (2014) Coronin 1 regulates cognition and behavior through modulation of cAMP/protein kinase A signaling. *PLoS Biol.* **12**, e1001820.

Kreis P. and Barnier J. V. (2009) PAK signalling in neuronal physiology. *Cell. Signal.* **21**, 384–393.

Lagenaur C., Kunemund V., Fischer G., Fushiki S. and Schachner M. (1992) Monoclonal M6 antibody interferes with neurite extension of cultured neurons. *J. Neurobiol.* **23**, 71–88.

Mattila P. K. and Lappalainen P. (2008) Filopodia: molecular architecture and cellular functions. *Nat. Rev. Mol. Cell Biol.* **9**, 446–454.

Michibata H., Okuno T., Konishi N. *et al.* (2008) Inhibition of mouse GPM6A expression leads to decreased differentiation of neurons derived from mouse embryonic stem cells. *Stem Cells Dev.* **17**, 641–651.

Mishima M. and Nishida E. (1999) Coronin localizes to leading edges and is involved in cell spreading and lamellipodium extension in vertebrate cells. *J. Cell Sci.* **112**(Pt 17), 2833–2842.

Mita S., deMonasterio-Schrader P., Funfschilling U., Kawasaki T., Mizuno H., Iwasato T., Nave K. A., Werner H. B. and Hirata T. (2015) Transcallosal projections require glycoprotein M6-dependent neurite growth and guidance. *Cereb. Cortex.* **25**, 4111–4125.

Moissoglu K., Slepchenko B. M., Meller N., Horwitz A. F. and Schwartz M. A. (2006) In vivo dynamics of Rac-membrane interactions. *Mol. Biol. Cell* **17**, 2770–2779.

Monteleone M. C., Adrover E., Pallares M. E., Antonelli M. C., Frasch A. C. and Brocco M. A. (2014) Prenatal stress changes the

glycoprotein GPM6A gene expression and induces epigenetic changes in rat offspring brain. *Epigenetics* **9**, 152–160.

Mukobata S., Hibino T., Sugiyama A., Urano Y., Inatomi A., Kanai Y., Endo H. and Tashiro F. (2002) M6a acts as a nerve growth factor-gated Ca(2 +) channel in neuronal differentiation. *Biochem. Biophys. Res. Commun.* **297**, 722–728.

Nakayama A. Y., Harms M. B. and Luo L. (2000) Small GTPases Rac and Rho in the maintenance of dendritic spines and branches in hippocampal pyramidal neurons. *J. Neurosci.* **20**, 5329–5338.

Nal B., Carroll P., Mohr E. *et al.* (2004) Coronin-1 expression in T lymphocytes: insights into protein function during T cell development and activation. *Int. Immunol.* **16**, 231–240.

Ojeda V., Castro-Castro A. and Bustelo X. R. (2014) Coronin1 proteins dictate rac1 intracellular dynamics and cytoskeletal output. *Mol. Cell. Biol.* **34**, 3388–3406.

Palamidessi A., Frittoli E., Garre M. *et al.* (2008) Endocytic trafficking of Rac is required for the spatial restriction of signaling in cell migration. *Cell* **134**, 135–147.

Pieters J., Muller P. and Jayachandran R. (2013) On guard: coronin proteins in innate and adaptive immunity. *Nat. Rev. Immunol.* **13**, 510–518.

Ridley A. J., Paterson H. F., Johnston C. L., Diekmann D. and Hall A. (1992) The small GTP-binding protein rac regulates growth factor-induced membrane ruffling. *Cell* **70**, 401–410.

Roussel G., Trifilieff E., Lagenaur C. and Nussbaum J. L. (1998) Immunoelectron microscopic localization of the M6a antigen in rat brain. *J. Neurocytol.* **27**, 695–703.

Rybakin V. and Clemen C. S. (2005) Coronin proteins as multifunctional regulators of the cytoskeleton and membrane trafficking. *BioEssays*, **27**, 625–632.

Scorticati C., Formoso K. and Frasch A. C. (2011) Neuronal glycoprotein M6a induces filopodia formation via association with cholesterol-rich lipid rafts. *J. Neurochem.* **119**, 521–531.

Sekino Y., Kojima N. and Shirao T. (2007) Role of actin cytoskeleton in dendritic spine morphogenesis. *Neurochem. Int.* **51**, 92–104.

Sells M. A., Knaus U. G., Bagrodia S., Ambrose D. M., Bokoch G. M. and Chernoff J. (1997) Human p21-activated kinase (Pak1) regulates actin organization in mammalian cells. *Curr. Biol.* **7**, 202–210.

Subauste M. C., Von Herrath M., Benard V., Chamberlain C. E., Chuang T. H., Chu K., Bokoch G. M. and Hahn K. M. (2000) Rho family proteins modulate rapid apoptosis induced by cytotoxic T lymphocytes and Fas. *J. Biol. Chem.* **275**, 9725–9733.

Suo D., Park J., Harrington A. W., Zweifel L. S., Mihalas S. and Deppmann C. D. (2014) Coronin-1 is a neurotrophin endosomal effector that is required for developmental competition for survival. *Nat. Neurosci.* **17**, 36–45.

Suzuki K., Nishihata J., Arai Y., Honma N., Yamamoto K., Irimura T. and Toyoshima S. (1995) Molecular cloning of a novel actin-binding protein, p57, with a WD repeat and a leucine zipper motif. *FEBS Lett.* **364**, 283–288.

Swaminathan K., Muller-Taubenberger A., Faix J., Rivero F. and Noegel A. A. (2014) A Cdc42- and Rac-interactive binding (CRIB) domain mediates functions of coronin. *Proc. Natl Acad. Sci. USA* **111**, E25–E33.

Vadodaria K. C., Brakebusch C., Suter U. and Jessberger S. (2013) Stage-specific functions of the small Rho GTPases Cdc42 and Rac1 for adult hippocampal neurogenesis. *J. Neurosci.* **33**, 1179–1189.

Wu D. F., Koch T., Liang Y. J., Stumm R., Schulz S., Schroder H. and Hollt V. (2007) Membrane glycoprotein M6a interacts with the micro-opioid receptor and facilitates receptor endocytosis and recycling. *J. Biol. Chem.* **282**, 22239–22247.

Yan Y., Lagenaur C. and Narayanan V. (1993) Molecular cloning of M6: identification of a PLP/DM20 gene family. *Neuron* **11**, 423–431.

Yan Y., Narayanan V. and Lagenaur C. (1996) Expression of members of the proteolipid protein gene family in the developing murine central nervous system. *J. Comp. Neurol.* **370**, 465–478.

Yan M., Collins R. F., Grinstein S. and Trimble W. S. (2005) Coronin-1 function is required for phagosome formation. *Mol. Biol. Cell* **16**, 3077–3087.

Zhang H., Webb D. J., Asmussen H. and Horwitz A. F. (2003) Synapse formation is regulated by the signaling adaptor GIT1. *J. Cell Biol.* **161**, 131–142.

Zhang H., Webb D. J., Asmussen H., Niu S. and Horwitz A. F. (2005) A GIT1/PIX/Rac/PAK signaling module regulates spine morphogenesis and synapse formation through MLC. *J. Neurosci.* **25**, 3379–3388.

Zhao J., Iida A., Ouchi Y., Satoh S. and Watanabe S. (2008) M6a is expressed in the murine neural retina and regulates neurite extension. *Mol. Vis.* **14**, 1623–1630.

